normal thyroid pertechnetate image or a thyroid image with a cold area corresponding to the area with increased focal uptake with tetrofosmin and sestamibi supported the parathyroid adenoma conclusion. Moreover, most parathyroid adenoma patients are elderly women, among whom irregular structure in the thyroid gland is a frequent phenomenon. Therefore, though not experienced in this study, thyroid scintigraphy may also eliminate false-positives caused by misinterpretation of tetrofosmin or sestamibi uptake in thyroid adenomas. In accordance with the recommendations from Hindie et al. (*4*) and Rossitch et al. (*7*), knowledge of the thyroid anatomy should improve the scintigraphic interpretation. Hence, irrespective of which of the two parathyroid preparations that is preferred, we strongly recommend that thyroid scintigraphy be included in the procedure.

Two of the 4 false-negative scintigraphic results were from investigations on patients with relatively small parathyroid adenomas: 0.16 and 0.23 g (Table 2). The patient with the 0.16-g adenoma had a thyroid scintigram indicating moderate multinodular goiter, while the other had a completely normal thyroid gland. A third patient with negative scintigraphy had a large adenoma of 1.37 g situated behind a multinodular goiter. When the scintigrams of this patient were revised postoperatively, we realized that the adenoma actually was visible.

Further investigations are in progress in our laboratory, with the intention to improve the image resolution and to find a simple and reliable same-day procedure for parathyroid scintigraphy with ^{99m}Tc-labeled tetrofosmin and thyroid scintigraphy with ^{99m}Tc-pertechnetate.

CONCLUSION

Tetrofosmin is an alternative to sestamibi for parathyroid scintigraphy. However, among the 16 patients in this study, the thyroid-parathyroid differential washout of sestamibi previously reported by other authors was never observed with tetrofosmin. Moreover, differential washout of sestamibi was not seen in 5 of 11 scintigraphically positive adenomas in the neck, and is, therefore, not a reliable diagnostic criterion. Irrespective of the preparation preferred for parathyroid visualization–sestamibi or tetrofosmin–combination with thyroid scintigraphy seems mandatory. Further studies are necessary to optimize the procedure for scintigraphic detection of parathyroid lesions.

ACKNOWLEDGMENTS

We thank Signe Elise Tjønneland and the technical staff of the Section of Nuclear Medicine, Rikshospitalet, The National Hospital of Norway, for expert technical assistance.

REFERENCES

1. Coakley AJ, Kettle AG, Wells CP, O'Doherty MJ, Collings REC. Technetium-99m-sestamibi: a new agent for parathyroid imaging. *Nucl Med Commun* 1989;10:791–794.
2. O'Doherty MJ, Kettle AG, Wells P, Collins REC, Coakley AJ. Parathyroid imaging with technetium-99m-sestamibi: preoperative localization and tissue uptake studies. *J Nucl Med* 1992;33:313–318.
3. Thule P, Thakore K, Vansant J, McGarity W, Weber C, Phillips LS. Preoperative localization of parathyroid tissue with ^{99m}Tc-sestamibi ^{123}I subtraction scanning. *J Clin Endocr Metab* 1994;78:77–82.
4. Hindie E, Melliere D, Simon D, Perlemuter L, Galle P. Primary hyperparathyroidism: is technetium 99m-sestamibi/iodine-123 subtraction scanning the best procedure to locate enlarged glands before surgery? *J Clin Endocr Metab* 1995;80:302–307.
5. Wei JP, Burke GJ, Mansberger AR Jr. Preoperative imaging of abnormal parathyroid glands in patients with hyperparathyroid disease using combination Tc-99m-pertechnetate and Tc-99m-sestamibi radionuclide scans. *Ann Surg* 1994;219:568–572.
6. Taillefer R, Boucher Y, Potvin C, Lambert R. Detection and localization of parathyroid adenomas in patients with hyperparathyroidism using a single radionuclide imaging procedure with technetium-99m-sestamibi (double phase study). *J Nucl Med* 1992;33:1801–1807.
7. Rossitch JC, Cowan RS, Ellis MB, Griffith RF. Technetium-99m-sestamibi for detection of parathyroid adenoma. Comparison of single and dual tracer imaging. *Clin Nucl Med* 1993;20:220–221.
8. Kelly D, Forster AM, Higley B, et al. Technetium-99m-tetrofosmin as a new radiopharmaceutical for myocardial perfusion imaging. *J Nucl Med* 1993;34:222–227.
9. Higley B, Smith FW, Smith T, et al. Technetium-99m-1,2-bis[bis(2-ethoxyethyl)phosphino]ethane: human biodistribution, dosimetry and safety of a new myocardial perfusion imaging agent. *J Nucl Med* 1993;34:30–38.
10. Ishibashi M, Nishida H, Kumabe T, Morita S, Matoba F, Nomura G, Hayabuchi N. Tc-99m-tetrofosmin. A new diagnostic tracer for parathyroid imaging. *Clin Nucl Med* 1995;20:902–905.

Comparison of Parathyroid Imaging with Technetium-99m-Pertechnetate/Sestamibi Subtraction, Double-Phase Technetium-99m-Sestamibi and Technetium-99m-Sestamibi SPECT

Charles C. Chen, Lawrence E. Holder, William A. Scovill, Ann M. Tehan and Donald S. Gann

Departments of Radiology and Surgery, University of Maryland Medical System, Baltimore, Maryland

The ability of ^{99m}Tc-pertechnetate/sestamibi subtraction, double-phase ^{99m}Tc-sestamibi and ^{99m}Tc-sestamibi SPECT imaging to localize abnormal parathyroid tissue was compared. **Methods:** Fifty-five consecutive patients had parathyroid imaging before surgery for hyperparathyroidism. Imaging consisted of ^{99m}Tc-pertechnetate pinhole images of the neck followed by ^{99m}Tc-sestamibi pinhole images of the neck and parallel-hole images of the neck and chest (early images). Within 2.5–4.0 hr later pinhole images of the neck, parallel-hole and SPECT images of the neck and chest were obtained (late images). Nodular foci of increased sestamibi activity were considered abnormal. **Results:** The sensitivity for abnormal parathyroid glands by visual comparison of early images and pertechnetate images was 72%–75%, late images and pertechnetate images was 73%–78% and double-phase (early and late) sestamibi images was 62%–65%; computer subtraction of pertechnetate from early images was 71%–74%; and SPECT imaging was 79%. The sensitivity for parathyroid adenomas was 89%–98%, while the sensitivity for hyperplastic parathyroid glands was only 47%–58%. **Conclusion:** Late imaging, computer subtraction and SPECT may not be necessary since they provided only marginal improvements on visual comparison of early sestamibi with pertechnetate images. Double-phase sestamibi imaging was less sensitive, so baseline thyroid imaging with pertechnetate is recommended.

Key Words: parathyroid; hyperparathyroidism; technetium-99m-sestamibi; technetium-99m-MIBI

J Nucl Med 1997; 38:834–839

Received Jul. 22, 1996; revision accepted Nov. 6, 1996.

For correspondence or reprints contact: Charles C. Chen, MD, Department of Radiology, Saint Francis Medical Center, 530 NE Glen Oak Ave., Peoria, IL 61637.

The accepted radionuclide method for imaging abnormal parathyroid tissue was the dual-tracer subtraction technique using ^{99m}Tc-pertechnetate and ^{201}Tl thallous chloride (*1,2*). However, since the introduction of ^{99m}Tc-sestamibi as a parathyroid imaging agent (*3,4*), various imaging protocols have been introduced (*3*). The different protocols can be categorized into the single-tracer double-phase (early and late) ^{99m}Tc-sestamibi imaging technique versus the dual-tracer subtraction techniques of ^{99m}Tc-sestamibi/^{123}I iodine or ^{99m}Tc-sestamibi/^{99m}Tc-pertechnetate.

Preliminary reports suggested that the sestamibi methods were equal or superior to the ^{99m}Tc-pertechnetate/^{201}Tl subtraction technique (*3*). However, there have been few direct comparisons of the single-tracer and dual-tracer sestamibi techniques. The current study presents the results of an imaging protocol that evaluated both single-tracer and dual-tracer techniques, as well as SPECT.

MATERIALS AND METHODS

Patients

Sixty-six consecutive patients referred to two experienced endocrine surgeons at the University of Maryland Medical System from March 1993 to October 1995 had parathyroid imaging before surgery for hyperparathyroidism. Of these patients, 11 declined surgery. The remaining 55 patients had surgical cures and were included in this study. One surgeon performed 28 and the other surgeon performed 27 of the operations.

Imaging Protocol

Ten to 15 min after injection of 74–111 MBq (2–3 mCi) ^{99m}Tc-pertechnetate, 5-min pinhole images of the neck were obtained. Without moving the patient, 740–925 MBq (20–25 mCi) ^{99m}Tc-sestamibi were injected followed by sequential 5-min pinhole images of the neck for a total of 30 min and a 5-min parallel-hole image of the neck and chest (early images). Within 2.5–4.0 hr later, a 5-min pinhole image of the neck, a 5-min parallel-hole image of the neck and chest and SPECT images (64 × 64 matrix, 64 steps, 20 sec per step) were obtained (late images). Computer subtraction of the 5-min pinhole pertechnetate images from the 5-min pinhole images at 30 min postinjection of ^{99m}Tc-sestamibi were performed.

Scan Interpretations

Interpretation of scintigraphic images was performed by a nuclear medicine physician blinded to the surgical results, initially comparing the pertechnetate images with the early, late, computer-subtracted and SPECT sestamibi images. The early and late images were then reanalyzed without the benefit of the ^{99m}Tc-pertechnetate images 3 mo later.

All images were digital and displayed on a computer workstation for analysis in random order. ROIs were drawn over areas of increased uptake corresponding to abnormal parathyroid tissue and compared to an ROI over normal thyroid parenchyma. Abnormal parathyroid/normal thyroid sestamibi uptake ratios were then calculated from early and late planar images.

Physiologic Criteria for Abnormal Parathyroid Tissue

Foci of increased activity identified on sestamibi images in excess of that seen on pertechnetate images were considered positive for abnormal parathyroid tissue. Images were interpreted as having definite, suggestive, equivocal and absent foci of abnormal parathyroid tissue uptake. For correlation with surgical and pathological results, definite and suggestive foci were considered positive, while equivocal and absent foci were considered negative.

When early and late (double-phase) planar sestamibi images were compared to each other without the information provided by pertechnetate images, foci of activity were considered positive if they were increased relative to thyroid tissue on early or late images, or both.

Anatomic Criteria for Abnormal Parathyroid Tissue

Nodular foci of sestamibi uptake clearly separate from the thyroid gland were considered abnormal. These foci need not have uptake greater than normal thyroid tissue to be considered positive. SPECT can help to isolate foci of parathyroid tissue from superimposed thyroid tissue. However, due to the spacial resolution limits of SPECT imaging, nodules of abnormal parathyroid tissue may manifest as only focal bulges in the contours of the thyroid gland.

Statistical Analysis

All data are expressed as mean ± 1 s.d. Estimates of specificity were based on the assumption that each patient had four parathyroid glands plus any ectopic parathyroid glands identified at surgery. Paired Student's t-tests were used to compare parathyroid/thyroid sestamibi uptake ratios.

RESULTS

Of the 55 patients who had surgical cures, 46 had primary hyperparathyroidism, eight had secondary hyperparathyroidism (end-stage renal disease) and one had tertiary hyperparathyroidism (end-stage renal disease but had a renal transplant). Twenty (36%) were men, and 35 (63%) were women. The men were 52 ± 12 yr old (range 30–77 yr), and the women were 55 ± 14 yr old (range 27–79 yr).

The mean serum calcium decreased from 11.2–9.1 mg/dl after surgery in patients with primary hyperparathyroidism and from 10.7–7.6 mg/dl in patients with secondary hyperparathyroidism. The mean serum phosphate levels increased from 2.6–3.3 mg/dl in primary hyperparathyroidism patients and decreased in secondary hyperparathyroidism patients from 7.3–6.5 mg/dl.

Forty-eight (87%) of the 55 patients were evaluated before initial surgery. Forty-one patients had primary hyperparathyroidism, six had secondary hyperparathyroidism and one patient had tertiary hyperparathyroidism. There were 17 men and 31 women. The men were 54 ± 12 yr old (range 30–77 yr), and the women were 56 ± 14 yr old (range 27–79 yr). One patient had a mixed papillary-follicular thyroid carcinoma that was visible as a hypofunctioning mass on both the pertechnetate and sestamibi images (Fig. 1)

The other seven (13%) patients were referred for reoperative surgery. Five had primary hyperparathyroidism, and two had secondary hyperparathyroidism. There were three men and four women, ages 42 ± 9 yr old (range 31–60 yr). Two of these patients were found to have ectopic parathyroid activity on imaging, and parathyroid adenomas were excised. One patient was found to have a parathyroid carcinoma involving the left thyroid gland (Fig. 2). One patient had MEN I syndrome and was found to have a 400-mg hyperplastic parathyroid gland that also was visible on imaging. The other three patients were found to have small parathyroid adenomas less than 100 mg in size (two of these were visible on imaging). The smallest parathyroid adenoma detected on imaging was 88 mg. The smallest hyperplastic parathyroid gland identified was 130 mg.

The results of planar sestamibi imaging with and without a ^{99m}Tc-pertechnetate image in 55 patients who had surgery are listed in Table 1. There were an estimated 227 possible parathyroid glands in this group of patients, four per person in 55 patients and seven ectopic parathyroid adenomas.

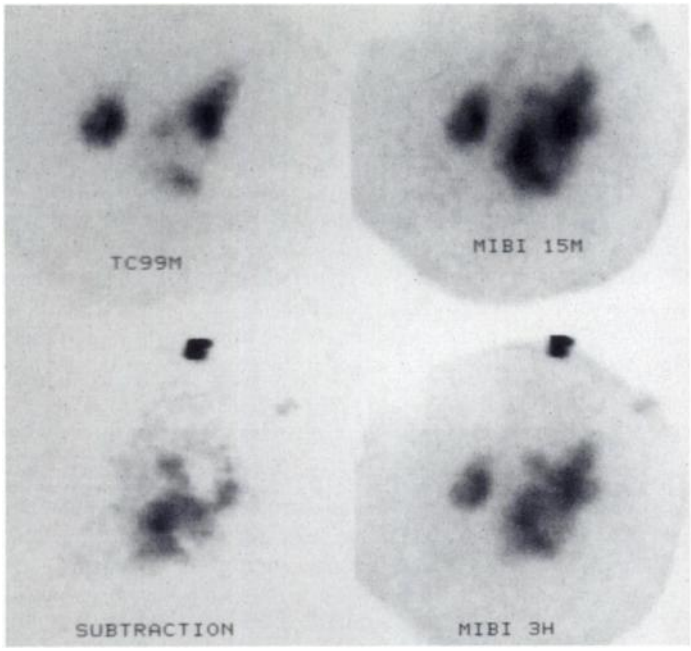

FIGURE 1. Patient with a thyroid carcinoma in the left lower thyroid lobe (note the hypofunctioning mass in the lateral left lower lobe) and a parathyroid adenoma just medial to the carcinoma (activity seen medial to the hypofunctioning mass on the ^{99m}Tc-sestamibi images). (Upper left) Technetium-99m-pertechnetate image, (upper right) early ^{99m}Tc-sestamibi image, (lower left) computer-subtraction image and (lower right) late ^{99m}Tc-sestamibi image.

Only the last 49 patients had SPECT imaging in addition to planar imaging. A comparison of planar and SPECT imaging in this subgroup of patients is shown in Table 2. There were an estimated 202 possible parathyroid glands, four per person in 49 patients and six ectopic parathyroid adenomas.

Nodular foci of increased sestamibi uptake corresponding to abnormal parathyroid tissue were usually noticeable by 15–20 min postinjection, but many were visible within 5 min postinjection. Parathyroid/normal thyroid tissue activity ratios were quantitatively determined in 39 patients in whom complete

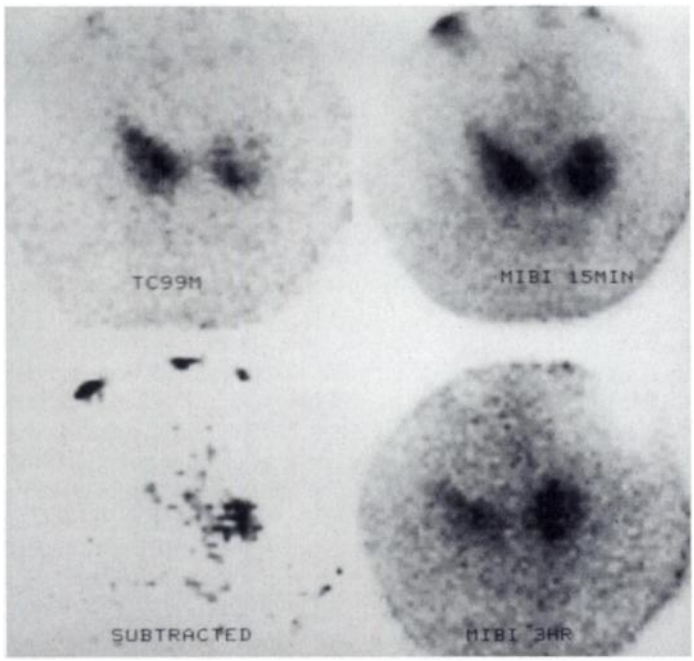

FIGURE 2. Patient with a parathyroid carcinoma involving the left upper thyroid gland. (Upper left) Technetium-99m-pertechnetate image, (upper right) early ^{99m}Tc-sestamibi image, (lower left) computer-subtraction image and (lower right) late ^{99m}Tc-sestamibi image.

TABLE 1
Planar Sestamibi Images with and without Pertechnetate Images Correlated with Surgical Findings

	Sens*/Spec†	No.	Early images	Late images	Subtr
Pertechnetate scan available	AD or HG*	82	72% (59)	73% (60)	71% (58)
	AD*	44	93% (41)	93% (41)	89% (39)
	HG*	38	47% (18)	50% (19)	50% (19)
	Ectopic AD*	7	85% (6)	85% (6)	71% (5)
	Normal†	145	92% (134)	93% (135)	94% (137)
Pertechnetate scan not available	AD or HG*	82	65% (53)	62% (51)	
	AD*	44	81% (36)	77% (34)	
	HG*	38	45% (17)	45% (17)	
	Ectopic AD*	7	85% (6)	85% (6)	
	Normal†	145	93% (135)	93% (135)	

*Sens = sensitivity; †Spec = specificity; AD = parathyroid adenomas; HG = hyperplastic parathyroid glands; No. = total numbers of glands (numbers in parentheses are numbers of glands detected on images); Subtr = computer subtraction of [^{99m}Tc]pertechnetate images from early sestamibi images.

(both early and late imaging) computerized data were available. A summary of the ratios is presented in Table 3 and Figure 3 (early images represent the 15 min postinjection images, late images represent the 2.5–4.0 hr postinjection images). Technetium-99m-sestamibi had variable uptake and washout in parathyroid tissue relative to normal thyroid tissue. Nodules with parathyroid/thyroid ratios less than or equal to 1.0 could still be visible if they were separated from thyroid tissue by a margin of decreased activity, such as ectopic parathyroid adenomas.

Pitfalls of Imaging

There was rapid washout of sestamibi from several parathyroid adenomas and hyperplastic parathyroid glands. In two patients with solitary parathyroid adenomas, the adenomas could not be clearly identified on late images but were visible on early images. Figure 4 illustrates one of these patients.

A major pitfall of parathyroid imaging in patients with multiple abnormal parathyroid glands was that there was a tendency to identify only the largest gland with the highest amount of activity. Figure 5 shows a patient who had two parathyroid adenomas, the right one was 802 mg and the left was 382 mg, but only the right gland was clearly identified on images.

Figure 6 demonstrates a patient with four hyperplastic parathyroid glands (3 g, 1.6 g, 1.1 g and 233 mg), but only the largest 3-g left upper gland was clearly identified and was misinterpreted as a solitary parathyroid adenoma. However, had the clinical history of end-stage renal disease in this patient been known before image interpretation, this could have been

TABLE 2
Planar and SPECT Sestamibi Images with Pertechnetate Images Correlated with Surgical Findings

Sens*/Spec†	No.	Early images	Late images	Subtr	SPECT
AD or HG*	73	75% (55)	78% (57)	74% (54)	79% (58)
AD*	40	95% (38)	98% (39)	90% (36)	98% (39)
HG*	33	52% (17)	55% (18)	55% (18)	58% (19)
Ectopic AD*	6	100% (6)	100% (6)	83% (5)	100% (6)
Normal†	129	91% (117)	92% (118)	94% (121)	91% (117)

*Sens = sensitivity; †Spec = specificity; AD = parathyroid adenomas; HG = hyperplastic parathyroid glands; No. = total numbers of glands (numbers in parentheses are numbers of glands detected on images); Subtr = computer subtraction of [^{99m}Tc]pertechnetate images from early sestamibi images.

TABLE 3
Parathyroid Adenoma/Thyroid Activity Ratios

Pattern	No.	Early ratio (range)	Late ratio (range)	P values
AD washin	15	1.09 ± 0.19 (0.75–1.45)	1.32 ± 0.35 (0.91–2.04)	<0.003
AD persist	3	1.09 ± 0.14 (0.94–1.21)	1.09 ± 0.13 (0.95–1.21)	ns
AD washout	9	1.27 ± 0.14 (1.10–1.54)	1.11 ± 0.11 (0.99–1.26)	<0.002
HG washin	9	1.09 ± 0.24 (0.77–1.37)	1.34 ± 0.17 (1.10–1.56)	<0.001
HG persist	1	0.97	0.98	ns
HG washout	6	1.17 ± 0.36 (0.63–1.58)	1.08 ± 0.38 (0.53–1.44)	<0.013
ECT AD washin	2	0.78 ± 0.40 (0.75–0.80)	1.21 ± 0.20 (1.07–1.35)	ns
ECT AD persist	3	0.54 ± 0.11 (0.44–0.65)	0.54 ± 0.10 (0.45–0.64)	ns

AD = parathyroid adenomas; HG = hyperplastic parathyroid glands; ECT = ectopic; sestamibi activity on late images relative to early images (washin = increased activity, washout = decreased activity, persist = equal activity).

prevented, since patients with secondary hyperparathyroidism most often have hyperplastic parathyroid glands (*3*).

Computer subtraction erroneously excluded a 327-mg parathyroid adenoma apparently because of superimposed activity in a thyroid adenoma (Fig. 7). At surgery, the parathyroid adenoma was extrathyroidal behind the lower pole of the right thyroid lobe. On imaging there was a focal area of increased uptake overlying the right lower thyroid gland on both the ^{99m}Tc-pertechnetate and ^{99m}Tc-sestamibi images consistent with a thyroid adenoma. SPECT imaging confirmed that there was increased activity in the lower pole of the right thyroid lobe but did not clearly identify a separate focus of parathyroid activity. An alternative explanation for this pattern could have been that the parathyroid adenoma also had increased ^{99m}Tc-pertechnetate uptake as reported by Leslie et al. (*5*).

Computer-subtraction image of one patient did not include an ectopic parathyroid adenoma in the field of view (Fig. 8, lower left). Subsequent larger field of view image of the neck and chest (Fig. 8, lower right) clearly demonstrated the ectopic parathyroid focus.

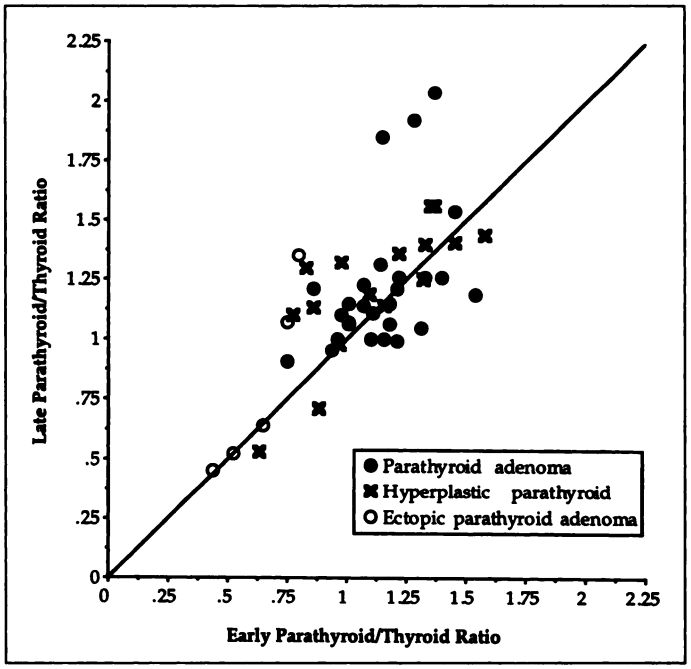

FIGURE 3. Graph correlating parathyroid/thyroid ratios of parathyroid adenomas, hyperplastic parathyroid glands and ectopic parathyroid glands on late versus early ^{99m}Tc-sestamibi images. Points above the line of identity represent parathyroid nodules that retained ^{99m}Tc-sestamibi on late images, while points below the line of identity represent parathyroid nodules that had ^{99m}Tc-sestamibi washout.

DISCUSSION

Contrary to the 90% sensitivity for detecting parathyroid adenomas with the double-phase technique reported by Taillefer et al. (*6*), the sensitivity of the double-phase technique in this study was only 77% to 81%. Variable sensitivities of the double-phase technique have been reported by others, ranging from 50% to 80% (*3*).

In contrast, the visual comparison of ^{99m}Tc-pertechnetate and ^{99m}Tc-sestamibi images had a sensitivity of 93% for detecting parathyroid adenomas (Table 1). Similar sensitivities have been reported by others (*3*), whether ^{99m}Tc-sestamibi images were compared to ^{99m}Tc-pertechnetate or ^{123}I images.

Thyroid gland images using ^{99m}Tc-pertechnetate are cheaper than images with ^{123}I. Both ^{99m}Tc-pertechnetate and ^{123}I images are superior to the "thyroid phase" or early ^{99m}Tc-sestamibi images at 15 min postinjection used in the double-phase ^{99m}Tc-sestamibi technique. Nodules of abnormal parathyroid tissue had increased uptake as early as 5 min postinjection of ^{99m}Tc-sestamibi and could be misinterpreted as thyroid nodules if only the 15-min ^{99m}Tc-sestamibi images were available for comparison.

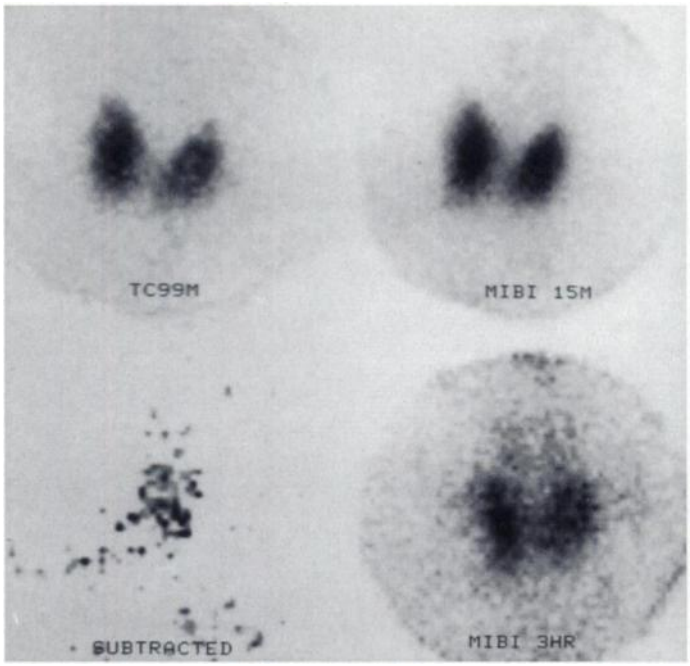

FIGURE 4. Patient with a parathyroid adenoma overlying the left upper thyroid gland that had rapid washout of ^{99m}Tc-sestamibi, visible on (upper right) the early ^{99m}Tc-sestamibi image but not on (lower right) the late ^{99m}Tc-sestamibi image. (Upper left) Technetium-99m-pertechnetate image and (lower left) computer-subtraction image.

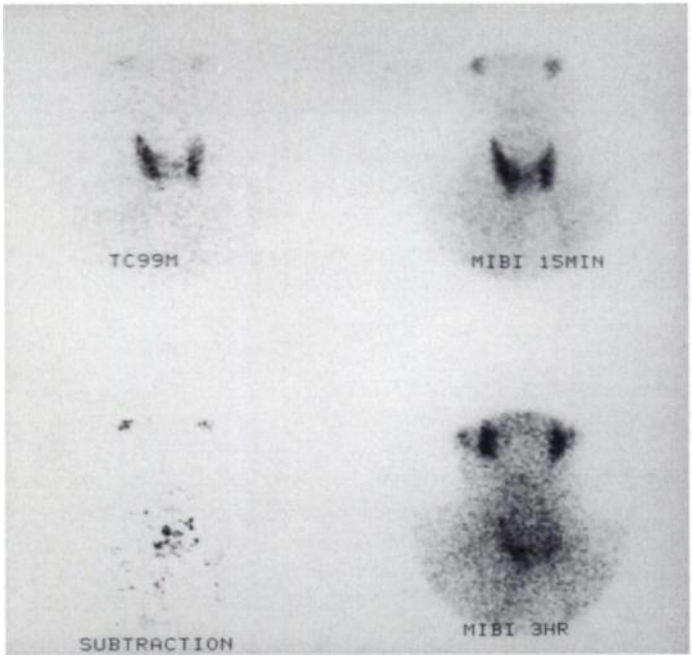

FIGURE 5. Patient with two parathyroid adenomas, the right one was 802 mg and the left was 382 mg, but only the right gland was identified on images. (Upper left) Technetium-99m-pertechnetate image, (upper right) early ^{99m}Tc-sestamibi image, (lower left) computer-subtraction image and (lower right) late ^{99m}Tc-sestamibi image.

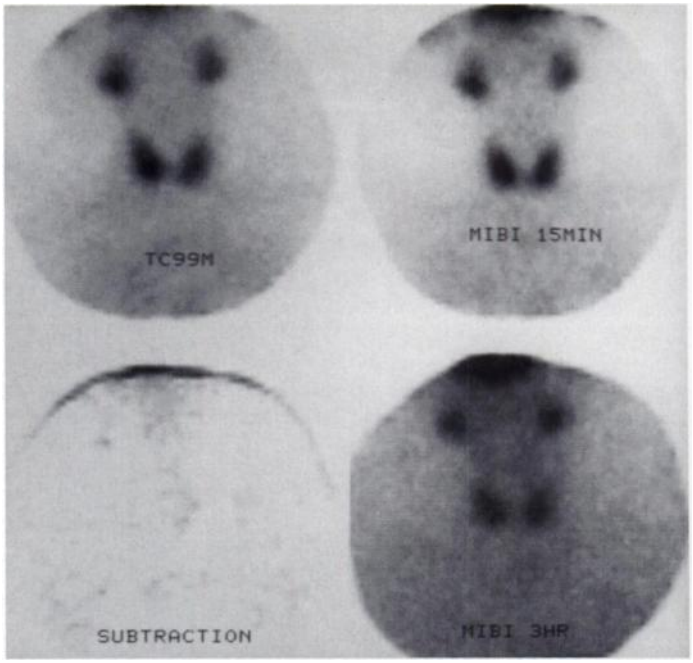

FIGURE 7. Computer subtraction erroneously excluded a 327-mg parathyroid adenoma apparently because of superimposed activity in a thyroid adenoma in the right lower lobe of the thyroid gland. (Upper left) Technetium-99m-pertechnetate image, (upper right) early ^{99m}Tc-sestamibi image, (lower left) computer-subtraction image and (lower right) late ^{99m}Tc-sestamibi image.

In addition, the rationale for double-phase imaging suggested by Taillefer et al. (*6*) of slower washout of ^{99m}Tc-sestamibi from parathyroid adenomas relative to thyroid tissue was not a universal physiologic phenomenon in our study group. Rapid washout of sestamibi from parathyroid adenomas and hyperplastic parathyroid glands in this series of patients was frequently identified, as documented by lower parathyroid/thyroid activity ratios in the late phase images compared to the early phase images (Table 3). Rapid washout also has been reported by others (*7,8*). As a result, abnormal parathyroid glands could be misinterpreted as thyroid nodules. Nodular foci with increased or separate sestamibi uptake relative to thyroid tissue on either the early or late images, or both, should be considered abnormal (*8*).

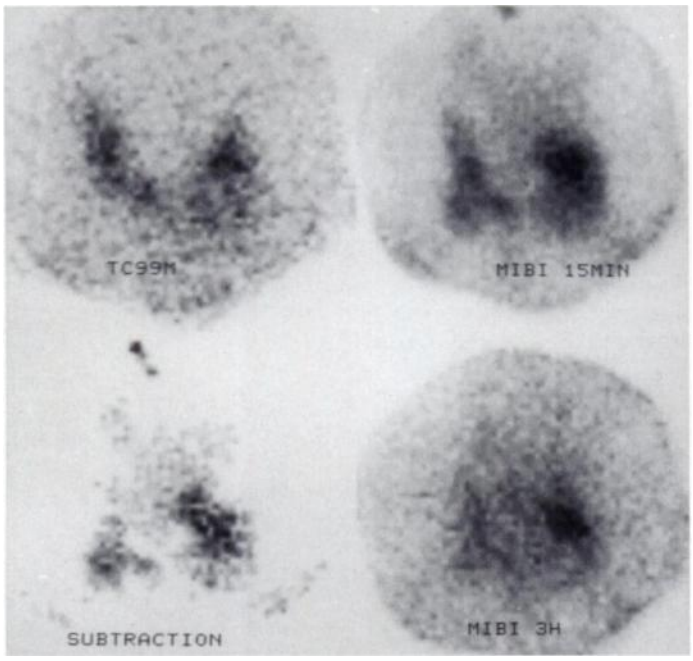

FIGURE 6. Patient with four hyperplastic parathyroid glands (3-g left upper gland, 1.6-g right upper gland, 1.1-g right lower gland and 233-mg left lower gland) and a clinical history of end stage renal disease. Only the largest (3-g left upper gland) was clearly identified. (Upper left) Technetium-99m-pertechnetate image, (upper right) early ^{99m}Tc-sestamibi image, (lower left) computer-subtraction image and (lower right) late ^{99m}Tc-sestamibi image.

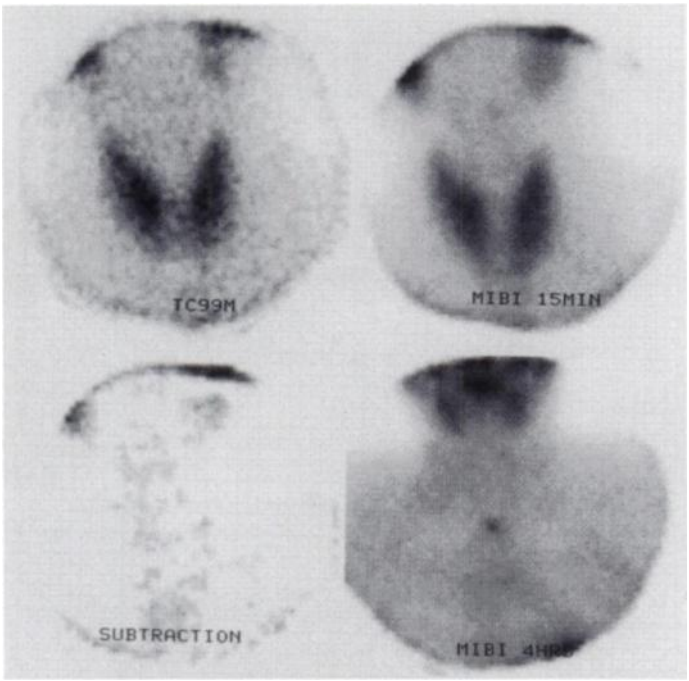

FIGURE 8. (Lower left) Computer-subtraction image, (upper left) ^{99m}Tc-pertechnetate image and (upper right) the early ^{99m}Tc-sestamibi image did not include an ectopic parathyroid adenoma in the field of view. The larger field of view ^{99m}Tc-sestamibi image of the neck and chest (lower right) clearly demonstrated the ectopic parathyroid adenoma in the midline, upper mediastinum.

Bérnard et al. (*7*) hypothesized that the rapid washout of ^{99m}Tc-sestamibi may be related to a decreased number of oxyphil cells, since their single case of a parathyroid adenoma with rapid washout lacked oxyphil cells. However, this has been questioned (*9*) and requires further study. Oxyphil cells usually found in parathyroid adenomas are rich in mitochondria, and mitochondrial content is the hypothesized mechanism of sestamibi retention in parathyroid tissue (*10*).

Late imaging, computer subtraction and SPECT imaging did not significantly increase the sensitivity or specificity of parathyroid imaging compared to the visual subtraction of ^{99m}Tc-pertechnetate from early ^{99m}Tc-sestamibi images. Therefore, they may not be necessary on a routine basis. Computer subtraction, late imaging and/or SPECT imaging may be reserved for any case where abnormal parathyroid tissue cannot be identified on initial images.

Computer subtraction, late imaging and SPECT imaging all have potential pitfalls but in individual patients may be helpful. Computer subtraction may highlight subtle areas of increased ^{99m}Tc-sestamibi uptake in small parathyroid nodules. Late images demonstrating foci with retention of ^{99m}Tc-sestamibi may be attributed more confidently to abnormal parathyroid tissue. If the foci of increased sestamibi uptake have rapid washout or washout at the same rate as normal thyroid tissue, then the foci have an intermediate probability for being abnormal parathyroid tissue, and surgical exploration of these areas may be helpful. SPECT helps to localize nodules in three dimensions that may be helpful to surgical planning. SPECT also can anatomically separate parathyroid nodules from overlapping thyroid tissue, again increasing the confidence that the nodules are abnormal parathyroid tissue.

A possible reason for why SPECT imaging had a lower (79%) sensitivity for detecting abnormal parathyroid tissue in this series of patients as opposed to the 94% sensitivity reported by Sfakianakis et al. (*11*) was that they performed early SPECT imaging. In contrast, only late SPECT imaging was performed in this study protocol for practical reasons. As a result of the decreased count density of late SPECT images and higher background image noise, abnormal foci were more difficult to identify. An alternative to SPECT imaging for practices without a SPECT camera would be to acquire high counting rate oblique images that decrease the overlap of thyroid and parathyroid tissues (*8*).

Late imaging alone is not recommended. Two of the parathyroid adenomas in the study group had rapid washout and were not visible on late images. In addition, late images occasionally had more overlapping activity in the neck strap muscles that obscured foci of parathyroid uptake.

Relying on computer-subtraction images alone would also be a mistake. Misregistration of images (position and counts normalization) and patient motion can make image interpretation difficult (*12,13*). Moreover, the smaller field of view of many computer subtraction protocols may miss ectopic parathyroid glands. So an image with a field of view large enough to include mediastinal ectopic foci should be in the image protocol (*14*).

Since an experienced surgeon will be able to localize up to 90%–95% of parathyroid adenomas during initial neck exploration, the role of preoperative imaging before initial surgeries has been questioned. However, failure to remove the abnormal parathyroid gland may result in significant patient morbidity (*6,14,15*). The potential of preoperative imaging is to decrease operative time and decrease the chances for surgical failure, such as locating small or ectopic parathyroid adenomas that could be missed during surgery.

Limiting surgeries to one side of the neck after a solitary abnormal gland has been localized by preoperative imaging is not recommended. Since only about 50% of the hyperplastic parathyroid glands were detected by scintigraphy, a patient with multiple hyperplastic parathyroid glands could be misinterpreted as having a solitary parathyroid adenoma and lead to surgical failure, similar to the experience of Sofferman et al. (*16*). However, imaging in conjunction with quick assays of intraoperative parathyroid hormone levels and surgery limited to the excision of visible parathyroid adenomas has promise (*11*).

Preoperative imaging was clinically useful. Identifying mediastinal or intrathyroidal parathyroid tissue altered surgical planning. The former changed the usual cervical surgery to a transmediastinal approach, and the latter alerted the surgeon to perform a thyroid lobectomy when an extrathyroidal parathyroid nodule could not be located (*16*).

Probably the most compelling reason to perform preoperative imaging was in patients who have failed prior surgery where the risk for ectopic parathyroid tissue is higher, up to 20% to 30% (*14*). Small parathyroid glands and ectopic parathyroid adenomas that either recurred or were missed after initial surgery were easily localized with imaging and excised for surgical cures in this report.

CONCLUSION

Late imaging, computer subtraction and SPECT may not be necessary since they provided only marginal improvements on visual comparison of early sestamibi and pertechnetate images. Double-phase sestamibi imaging was less sensitive, so baseline thyroid imaging with ^{99m}Tc-pertechnetate is recommended. Parathyroid adenomas including ectopic parathyroid adenomas were easily identified, but only about half of the hyperplastic parathyroid glands were visible.

REFERENCES

1. Goris ML, Basso LV, Keeling C. Parathyroid imaging. *J Nucl Med* 1991;32:887–889.
2. Fine EJ. Parathyroid imaging: its current status and future role. *Semin Nucl Med* 1987;17:350–359.
3. McBiles M, Lambert AT, Cote MG, Kim SY. Sestamibi parathyroid imaging. *Semin Nucl Med* 1995;25:221–234.
4. Coakley J, Kettle AG, Wells CP. Technetium-99m-sestamibi–a new agent for parathyroid imaging. *Nucl Med Commun* 1989;10:791–794.
5. Leslie WD, Riese KT, Guzman R, Dupont JO, Peterdy AE. Technetium-99m-pertechnetate uptake by intrathyroidal parathyroid adenoma. *J Nucl Med* 1996;37:861–862.
6. Taillefer R, Boucher Y, Potvin C, Lambert R. Detection and localization of parathyroid adenomas in patients with hyperparathyroidism using a single radionuclide imaging procedure with technetium-99m-sestamibi (double-phase study). *J Nucl Med* 1992;33:1801–1807.
7. Bérnard F, Lefebvre B, Beuvon F, Langlois MF, Bisson G. Rapid washout of technetium-99m-MIBI from a large parathyroid adenoma. *J Nucl Med* 1995;36:241–243.
8. Chen CC, Skarulis MC, Fraker DL, Alexander HR, Marx SJ, Spiegel AM. Technetium-99m-sestamibi imaging before reoperation for primary hyperparathyroidism. *J Nucl Med* 1995;36:2186–2191.
9. Staudenherz A, Kletter K, Leitha T. Rapid washout of technetium-99m-MIBI from a large parathyroid adenoma [Letter]. *J Nucl Med* 1995;36:1928.
10. Chiu ML, Kronauge JF, Piwnica-Worms D. Effect of mitochondrial and plasma membrane potentials on accumulation of hexakis (2-methoxyisobutylisonitrile) technetium (I) in cultured mouse fibroblasts. *J Nucl Med* 1990;31:1646–1653.
11. Sfakianakis GN, Irvin GL, Foss J, et al. Efficient parathyroidectomy guided by SPECT-MIBI and hormonal measurements. *J Nucl Med* 1996;37:798–804.
12. Sandrock D, Merino MJ, Norton JA, Neumann RD. Parathyroid imaging by Tc/Tl scintigraphy. *Eur J Nucl Med* 1989;16:607–613.
13. Liehn JC, Delisle MJ, Flament JB. Improvement of parathyroid Tl-Tc scintigraphy by using a new image subtraction method. *Eur J Nucl Med* 1988;14:184–189.
14. Rantis PC, Prinz RA, Wagner RH. Neck radionuclide scanning: a pitfall in parathyroid localization. *Am Surgeon* 1995;61:641–645.
15. Satava RM, Beahrs OH, Scholz DA. Success rate of cervical exploration for hyperparathyroidism. *Arch Surg* 1975;110:625–628.
16. Sofferman RA, Nathan MH, Fairbank JT, Foster RS, Krag DN. Preoperative technetium-99m-sestamibi imaging: paving the way to minimal-access parathyroid surgery. *Arch Otolaryngol Head Neck Surg* 1996;122:369–374.